



Article

CO₂ Capture over Activated Carbon Derived from Pulverized Semi-Coke

Jieying Jing^{1,2,3,*} , Zemin Zhao^{1,2}, Xuewei Zhang^{1,2}, Jie Feng^{1,2} and Wenying Li^{1,2} 

¹ State Key Laboratory of Clean and Efficient Coal Utilization, Taiyuan University of Technology, Taiyuan 030024, China; zhaozemin0630@link.tyut.edu.cn (Z.Z.); zhangxuewei0623@link.tyut.edu.cn (X.Z.); fengjie@tyut.edu.cn (J.F.); ying@tyut.edu.cn (W.L.)

² Key Laboratory of Coal Science and Technology, Taiyuan University of Technology, Ministry of Education, Taiyuan 030024, China

³ Shanxi-Zheda Institute of Advanced Materials and Chemical Engineering, Taiyuan 030000, China

* Correspondence: jingjieying@tyut.edu.cn; Tel./Fax: +86-351-6018453

Abstract: Pulverized semi-coke was employed as raw material to prepare activated carbon via steam activation and evaluated as a CO₂ adsorbent. The effects of the preparation parameters including demineralization, activation temperature, activation time and steam flow on the structure and performance of the synthesized activated carbon were investigated. It was found that the microporous structure of activated carbon was greatly influenced by demineralization order and activation conditions. Demineralization before activation significantly increased the microporous structure of the activated carbon, which was ascribed to the removal of the inorganic fraction. Compared to the commercial activated carbon, activated carbon obtained by employing 150 mL/min steam to treat the demineralized pulverized semi-coke at 700 °C for 70 min possessed a higher CO₂/N₂ selectivity of 34.4 and good cyclic performance, which was due to its narrow microporosity of 0.55 nm. Furthermore, it was proved that a pore size of smaller than 1 nm is favorable for CO₂ sorption.

Keywords: pulverized semi-coke; steam activation; activated carbon; CO₂ capture; CO₂/N₂ selectivity



Citation: Jing, J.; Zhao, Z.; Zhang, X.; Feng, J.; Li, W. CO₂ Capture over Activated Carbon Derived from Pulverized Semi-Coke. *Separations* **2022**, *9*, 174. <https://doi.org/10.3390/separations9070174>

Academic Editors: Bin Xu and Yu Gong

Received: 18 June 2022

Accepted: 11 July 2022

Published: 13 July 2022

Publisher's Note: MDPI stays neutral with regard to jurisdictional claims in published maps and institutional affiliations.



Copyright: © 2022 by the authors. Licensee MDPI, Basel, Switzerland. This article is an open access article distributed under the terms and conditions of the Creative Commons Attribution (CC BY) license (<https://creativecommons.org/licenses/by/4.0/>).

1. Introduction

The concentration of carbon dioxide (CO₂) in the atmosphere is gradually increasing due to rapid economic and industrial development. It is reported that the atmospheric CO₂ concentration increased from 280 ppm in the year 1800 to 414 ppm in 2021 [1], resulting in a global temperature rise of 1.2 °C and a series of global problems involving global warming, tropical storms, rising sea levels, etc. How to capture CO₂ reasonably and efficiently to achieve carbon neutrality is an urgent question for China. As is well established, coal-fired power plants account for about 75% of CO₂ emissions. Therefore, it is very important to investigate the capture of CO₂ in flue gas so as to reduce the greenhouse effect and build a sustainable ecological environment. Carbon capture and storage (CCS) is an effective technology to achieve carbon emission reduction in the short-to-medium term [2–4]. There are three typical types of CO₂ capture including pre-combustion, oxygen-rich combustion and post-combustion. The post-combustion CO₂ capture technology mainly involves capturing CO₂ gas from the post-combustion flue gas [5–7]. The key challenge of this technology is to find materials that have a high CO₂ capture capacity in conditions where the flow rate is high and with an atmospheric pressure with low partial pressure of CO₂ (3–20% by volume).

Currently, 30 wt% aqueous monoethanolamine (MEA) scrubbing is the most developed and advanced approach for capturing CO₂ in large-scale industrial projects because of its high CO₂ removal capacity of 87~100% [8]. However, this process has some drawbacks, such as high regeneration energy (3.8–4.2 GJ/t CO₂), proneness to degradation, toxicity of

amines and severe equipment corrosion [9–11]. Instead, the solid adsorption method to capture CO₂ has become one of promising alternative technologies owing to its advantages of a high CO₂ sorption capacity, high regeneration rate and simple operation process [12–14]. There are a variety of solid adsorbents, involving zeolites, activated carbon, metal organic frameworks (MOFs), silica gels, etc., of which activated carbon is thought to be one of the promising candidates for capturing CO₂ because of its good stability in moist conditions and excellent chemical and thermal stability [15,16].

Semi-coke is the solid by-product of the low rank coal pyrolysis at 500–700 °C. Because of the poor adhesive property of low rank coal, semi-coke is prone to cracking, resulting in pulverized semi-coke. There were reportedly around 76 million tons of semi-coke in 2020, and about 10% of semi-coke is pulverized to a small size (<3 mm), meaning it is generally burned or directly discarded. Considering the high fixed carbon content in pulverized semi-coke, activated carbon might be derived from pulverized semi-coke, which could achieve the high-value utilization of pulverized semi-coke. However, CO₂ is generally adsorbed on activated carbon in the form of physical adsorption and it is normally weak, which makes activated carbon sensitive to temperature and has a relatively poor selectivity. Current research mainly focuses on how to improve the interaction between CO₂ and adsorbents so as to enhance CO₂ selectivity. For instance, Serafin et al. synthesized a series of biomass-derived activated carbon. They found that the raw materials greatly affect the textural properties of the resulting activated carbon and their CO₂ capture performance [17]. Wang et al. used semi-coke to prepare activated carbon via potassium hydroxide (KOH) activation for aqueous tetracycline removal. They reported that the KOH dosage and pyrolysis temperature could tune the surface area of the resulting activated carbon [18]. Tian et al. prepared activated carbon by using low-rank coals and oxidized pellets as raw materials. They found that the activation condition greatly influenced the microstructure of the obtained activated carbon [19]. Heidarinejad et al. reviewed chemical activation agents for activated carbon preparation. It was found that the chemical activation agent determined the performance and applicability of activated carbon [20]. Thus, it is known that one effective way to enhance CO₂ selectivity is to adjust the pore structure of the activated carbon and increase its surface area, which was closely related to the raw materials, preparation method, activation conditions and so on.

When pulverized semi-coke is employed as the raw material, a simple activation process needs be chosen to adjust the porosity and the surface area of the activated carbon derived from pulverized semi-coke. The common activation methods include physical activation (CO₂ or H₂O as the activating agents) and chemical activation (KOH, zinc chloride (ZnCl₂), phosphoric acid (H₃PO₄), nitric acid (HNO₃), etc as the activating agents). The physical activation method is environmentally friendly and basically produces no pollutants compared with the chemical activation method [21]. The physical activation process generally involves two steps, that is, the raw material is first carbonized, and then the activation process is followed to obtain activated carbon. Since pulverized semi-coke is the solid by-product of low-rank coal pyrolysis and it has already undergone the carbonization process, it is reasonable to choose the physical activation method to prepare activated carbon.

Considering the high fixed carbon content in pulverized semi-coke, in this work, porous activated carbon with narrow microporosity was prepared using the steam activation method with pulverized semi-coke as the raw material so as to achieve the high-value utilization of pulverized semi-coke. Since the pore structure of the activated carbon was formed during the activation process, we placed emphasis on investigating how the preparation parameters involving demineralization, activation temperature, activation time and steam flow affected the structure and performance of the synthesized activated carbon. The potential application of the obtained activated carbon was evaluated as CO₂ adsorbent under a simulative post-combustion condition. The goal of this work was to prepare a type of economic and efficient activated carbon, and develop a new approach for utilizing pulverized semi-coke.

2. Experimental Section

2.1. Raw Materials

The pulverized semi-coke was obtained by pyrolyzing Hulunbel lignite at 650 °C. A temperature of 650 °C was selected because our previous work revealed that a high coal tar yield could be achieved at this temperature [22,23]. The proximate analysis and ultimate analysis of Hulunbel lignite and pulverized semi-coke are shown in Table 1. The particle size of pulverized semi-coke was 0.25–0.45 mm.

Table 1. Proximate and ultimate analysis of Hulunbel lignite and pulverized semi-coke.

Samples	Proximate Analysis w_{ad} (%)				Ultimate Analysis w_{daf} (%)				
	M	A	V	FC *	C	H	O *	N	S
Hulunbel Lignite	11.44	13.11	33.08	42.37	74.01	4.11	19.97	1.26	0.65
Pulverized semi-coke	4.77	18.95	17.04	59.24	81.50	3.03	14.22	0.82	0.43

*: by difference. M: Moisture, A: Ash, V: Volatiles, FC: Fixed Carbon.

2.2. Demineralization of Pulverized Semi-Coke

A conventional acid digestion step was conducted to remove ash from the samples. The desired amount of pulverized semi-coke was treated with 6 mol/L HCl at 70 °C for 2 h, then treated with HF at 70 °C for 4 h, and finally with 6 mol/L HCl at 70 °C for 2 h (1 g pulverized semi-coke per 10 mL solution) [24]. After acid washing, the materials were washed thoroughly by deionized water until the filtrate became neutral and dried for overnight at 110 °C under air atmosphere. The pulverized semi-coke raw material was denoted as SC, and the demineralized samples as DME.

2.3. Activated Carbon Preparation

Activated carbon was obtained using steam to activate the pulverized semi-coke at different activation conditions, and the effects of activation conditions including activation temperature, activation time and steam flow were investigated. Typically, 1.5 g of pulverized semi-coke or acid-washed pulverized semi-coke was placed in a fixed bed reactor and heated to activation temperature under an Ar atmosphere at a flow rate of 10 °C/min. When heating to the activation temperature (650–800 °C), different amounts of steam (50–200 mL/min) were introduced into the reactor. After activating at different timepoints (30–90 min), the reaction temperature was dropped to room temperature under the Ar atmosphere to obtain the activated carbon. The obtained samples were named based on their activation conditions and marked as AC-T-t-W (T: activation temperature, °C; t: activation time, min; W: steam flow, mL/min). For example, AC-700-70-150 refers to activated carbon obtained by employing 150 mL/min steam to treat pulverized semi-coke at 700 °C for 70 min. When conducting the optimization experiment of activated carbon preparation parameters, a pre-orthogonal experiment including 3 influencing factors (activation temperature, activation time and steam flow) was first performed, then a single factor analysis was conducted to further optimize the activation temperature, activation time and steam flow.

2.4. Activated Carbon Characterization

X-ray diffraction (XRD, Rigaku, Tokyo, Japan) was used to analyze the crystallographic structure of the samples. The scanning range was 10–80°, and the radiation was produced at 40 kV and 40 mA. The surface area and pore structure of the activated carbon was measured at −196 °C by nitrogen adsorption–desorption analysis on a physical adsorption instrument (JW-BK122W, JWGB, Beijing, China). The specimens were outgassed under vacuum at 250 °C for 4 h before analysis. DFT pore size analysis was also recorded on the same instrument at −196 °C. The micropore volume was determined according to the *t*-plot method [25]. The surface morphologies of the pulverized semi-coke and activated carbon were examined via scanning electron microscopy (SEM, HITACHI, Ibaraki, Japan).

The iodine value was generally used to represent the amount of micropores [26]. The iodine value was examined according to GB/T 7702.7-2008. Each sample was tested at least 3 times, and the experimental result was considered reliable only if the calculated relative deviation was within 5%.

2.5. CO₂ Uptake Measurement

CO₂ capture behaviors were measured using thermal gravimetric analyzer (TGA, NETZSCH, Selb, Germany) under ambient pressure. In a typical process, a 15 mg sample was heated to 120 °C under N₂ atmosphere and held for 10 min, then the temperature was decreased and kept at 40 °C. Adsorption was started via switching the gas to 15% CO₂ in N₂ (60 mL/min), and the temperature was maintained at 40 °C for 30 min, after which the sample was heated to 120 °C in N₂ (60 mL/min) to remove CO₂. The cyclic behavior of the selected adsorbent was also evaluated in a thermal gravimetric analyzer. Then, 100% N₂ was also used as feed gas for comparison. The total mass uptake (q) and CO₂ sorption capacity (n) were calculated using the following formula:

$$q(\text{wt.}\%) = \frac{m_{\text{ad}}}{m} \times 100 \quad (1)$$

$$n(\text{mmol/g}) = \frac{m_{\text{ad}}}{M_{\text{CO}_2} \times m} \times 1000 \quad (2)$$

where m_{ad} is the mass gain of the sample after adsorbing CO₂, mg; m is the initial mass of sample, mg; and M_{CO_2} is the molar mass of CO₂, 44 g/mol.

3. Results and Discussion

3.1. Influence of Demineralization on the Properties of the Activated Carbon

In order to investigate the influence of minerals in ash, different samples were prepared. If pulverized semi-coke (SC) was directly activated by steam at 700 °C for 70 min, the resulting activated carbon was marked as SC-AC. The demineralization order was also considered. The activated carbon derived from demineralizing SC-AC was denoted as SC-AC-DME; while an SC-DME-AC sample was obtained if the activated carbon was derived from first demineralizing SC, then proceeding to the activation process. Figure 1 presented the XRD patterns of different activated carbon samples. It was clear that the activated carbon without demineralization (SC-AC) contained many inorganic minerals, which was ascribed the loss of carbon and volatility during the activation process and resulted in the exposure of inorganic minerals. After demineralizing, the SC-AC-DME or SC-DME-AC sample had no diffraction peaks of inorganic minerals, which indicated that these minerals in pulverized semi-coke raw material could be effectively eliminated by acid treatment, which was not relevant to the demineralization order.

Considering that the CO₂ sorption capacity of the activated carbon had a direct relationship with its pore structure [27], the influence of demineralization on the pore structure of the activated carbon was investigated (Figure 2). Results showed that the N₂ adsorption/desorption curve of SC-DME-AC sample was similar to I isotherm. It implied that the SC-DME-AC sample possessed a well-developed microporous structure, which was intrinsically associated with the CO₂ sorption capacity at an atmospheric pressure [25,28]. Meanwhile, it was clear that the N₂ adsorption/desorption curves of SC-AC and SC-AC-DME were similar to II isotherm, indicating that their pore structures were mesoporous. Furthermore, the BET specific surface area (S_{BET}), the total pore volume (V_{t}), the micropore volume (V_{mic}), the ratio of V_{mic} and V_{t} and the iodine value exhibited the textural properties of different activated carbon samples, as presented in Table 2. It was clear that raw material SC possessed a lower specific surface area (120.5 m²/g), a small total pore volume of 0.11 cm³/g and its iodine value was 250.6 mg/g; after being activated by steam at 700 °C for 70 min, the specific surface area of SC-AC was 531.4 m²/g and the total pore volume and its iodine value increased to 0.37 cm³/g and 621.2 mg/g, respectively. The specific surface area, the total pore volume and the iodine value were

further enhanced after demineralization, which might be due to the opening of the clogged pores after removing inorganic mineral. It was interesting that the specific surface area of the SC-AC-DME sample was higher than that of SC-DME-AC, while the iodine value of the SC-AC-DME sample was lower than that of SC-DME-AC. Comparing the V_{mic} and V_t ratio of different samples, it was obvious that SC-DME-AC possessed the highest micropore ratio. It meant that the activated carbon obtained from first demineralizing SC, then proceeding to the activation process (SC-DME-AC) possessed a more microporous structure, which would be beneficial to the CO_2 adsorption. Thus, in the following study, all activated carbon was first demineralized before activation.

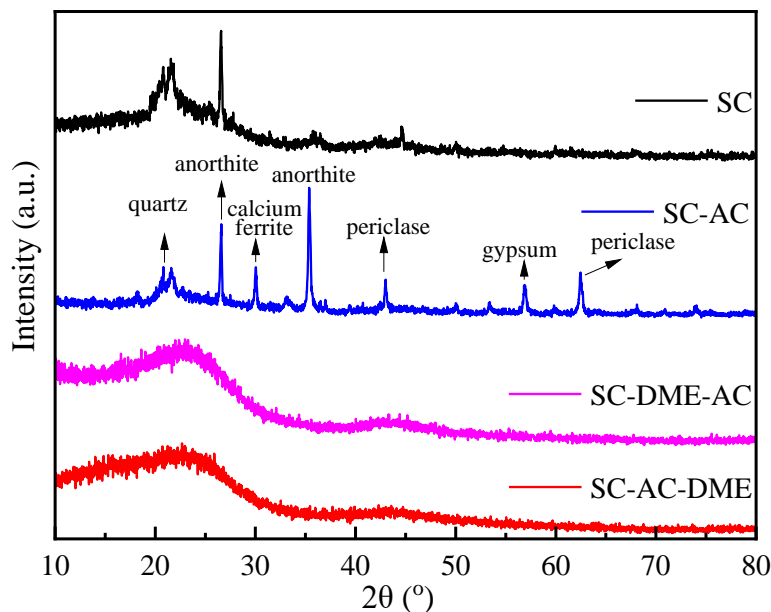


Figure 1. XRD patterns of different activated carbon samples. (quartz: SiO_2 , anorthite: $CaAl_2Si_2O_8 \cdot 4H_2O$, calcium ferrite: $Ca_{0.15}Fe_{2.85}O_4$, periclase: MgO , gypsum: $CaSO_4$).

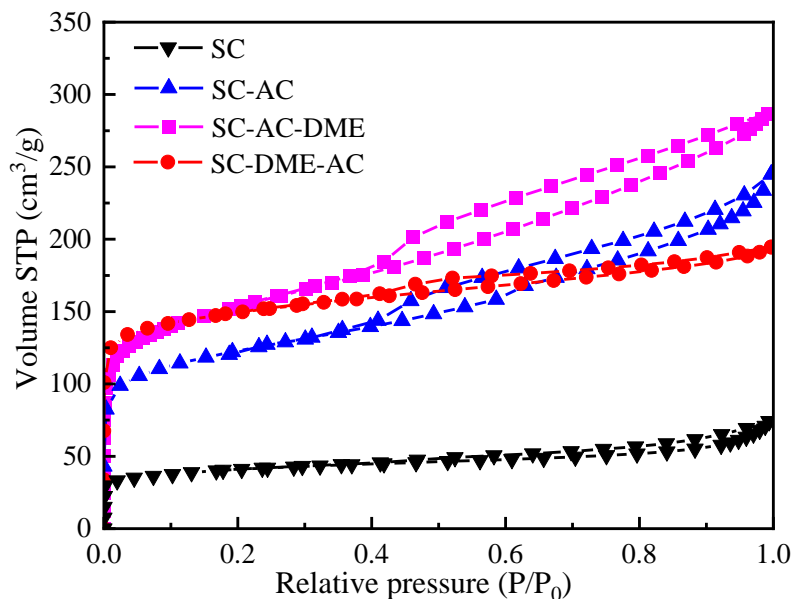


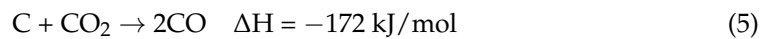
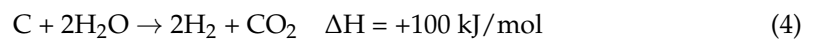
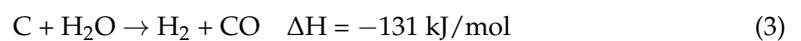
Figure 2. N_2 adsorption/desorption curves of different samples.

Table 2. The specific surface area and iodine value of different samples.

Samples	S _{BET} (m ² /g)	V _t (cm ³ /g)	V _{mic} (cm ³ /g)	Ratio V _{mic} :V _t	Iodine Value (mg/g)
SC	120.5	0.11	0.07	0.64	250.6
SC-AC	531.4	0.37	0.21	0.57	621.2
SC-AC-DME	620.6	0.44	0.27	0.61	705.2
SC-DME-AC	590.2	0.29	0.24	0.83	755.6

3.2. Optimization of Activated Carbon Preparation Parameters

The steam activation of the pulverized semi-coke led to the reaction between carbon and steam to generate gas and then form pores. The main chemical reactions are summarized as follows [29,30].



The reaction process could be divided into the following stages (Figure 3): the steam first diffused to the surface of pulverized semi-coke after demineralization, and then was adsorbed by the activated carbon atom (active site) to undergo a gasification reaction forming pores. The pore structure could be developed uniformly only if the steam diffusion rate was similar to the activation reaction rate, which was greatly determined by the activation conditions.

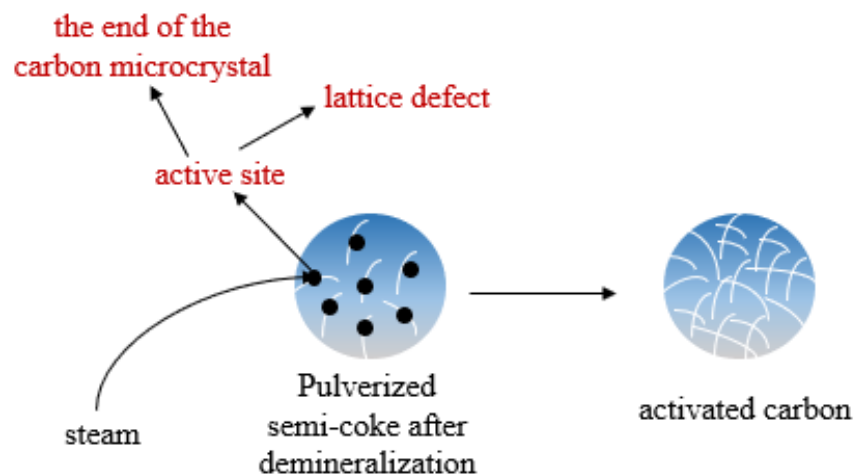


Figure 3. Steam activation pathway for semi-coke.

3.2.1. Optimization of Activation Temperature

The effect of the activation temperature on the property of activated carbon was studied when the steam flow rate was 150 mL/min and the activation time was 50 min. It is presented in Figure 4 that as the activation temperature increased, the specific surface area and iodine value first increased and then decreased. These trends were consistent with the published results [31]. It is known that the reaction between carbon and steam was endothermic. When the activation temperature was low, the reaction rate between carbon and steam was slow, and mainly non-organizational carbon such as the blocking tar in the channel reacted with steam, thus the porosity of the pulverized semi-coke did not change drastically. As the activation temperature increased, the reaction rate became faster. Studies [32] have shown that the reaction between steam and carbon does not evenly distribute across the entire semi-coke surface, but only in the active sites. For example, the end of the carbon microcrystal or lattice defect sites. Thus, steam spread into the

inside pore and reacted with pulverized semi-coke, producing the porous activated carbon. As the activation temperature was elevated from 700 °C to 750 °C, although the specific surface area was slightly increased, the iodine value decreased, which indicated that a high temperature was not conducive to the formation of micropores. When the activation temperature was too high, steam was prone to react with the surface carbon, not to diffuse into the inside pore. Because a microporous structure is preferred in CO₂ adsorption, the optimal activation temperature is 700 °C.

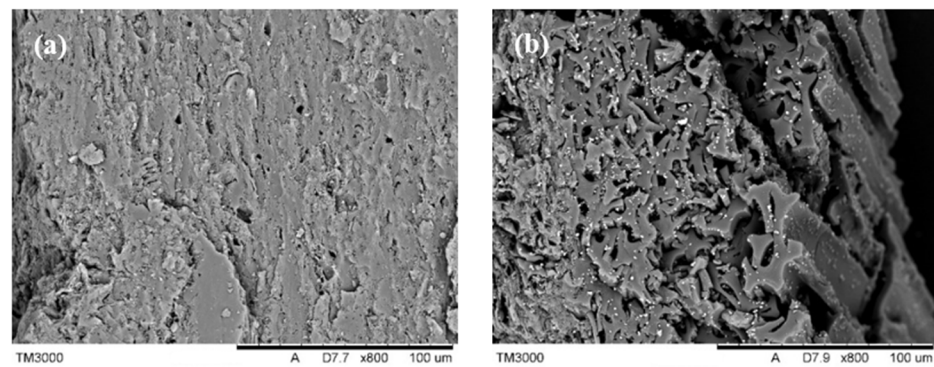


Figure 4. Influence of activation temperature on the textural property of the obtained sample.

3.2.2. Optimization of Activation Time

The influence of activation time on the property of activated carbon was studied when the steam flow rate was 150 mL/min and the activation temperature was 700 °C. As shown in Figure 5, when the activation time was short, the carbon in the pulverized semi-coke could not react sufficiently with steam; thus, it was hard to obtain activated carbon with the developed pore structure. As the activation time increased from 30 min to 70 min, the specific surface area increased from 408.1 m²/g to 613.2 m²/g, and the iodine value increased from 542.5 mg/g to 755.6 mg/g, indicating that the porosity of activated carbon was fully developed. However, when the activation time was prolonged, the specific surface area and iodine of the obtained activated carbon decreased. The increased activation time would destroy the micropore wall to form macropores—even causing carbon skeleton collapse—resulting in the decreased specific surface area and iodine value. Therefore, the optimal activation time was chosen as 70 min to obtain porous activated carbon from pulverized semi-coke.

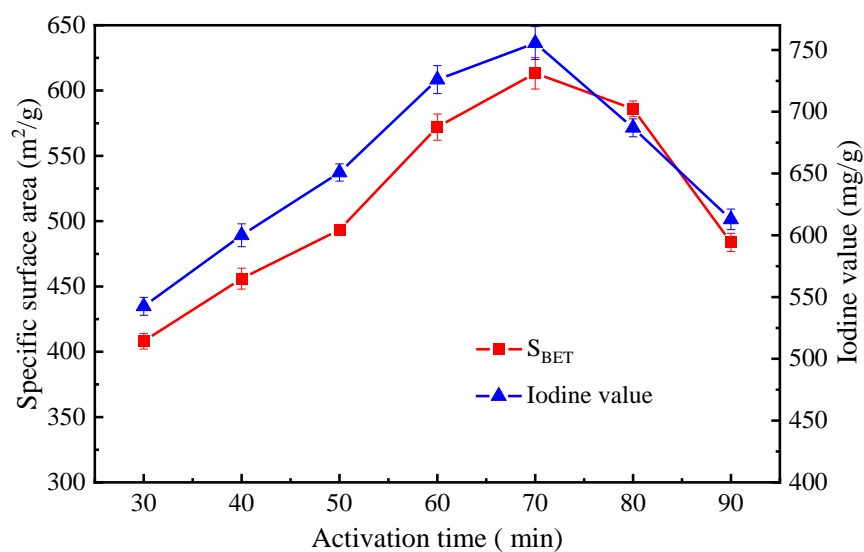


Figure 5. Effect of activation time on the textural property of the obtained sample.

3.2.3. Optimization of Steam Flow

The effect of steam flow on the property of activated carbon was studied when the activation temperature was 700 °C and the activation time was 70 min. As illustrated in Figure 6, the activation reaction rate accelerated with the increasing steam flow. This was advantageous to the activation reaction and the porosity of activated carbon. However, when the steam flow increased to 200 mL/min, the surface temperature of the materials decreased [33], leading to a lower reaction rate, which was not conducive to the formation of new pores. Thus, the optimal steam flow was determined as 150 mL/min.

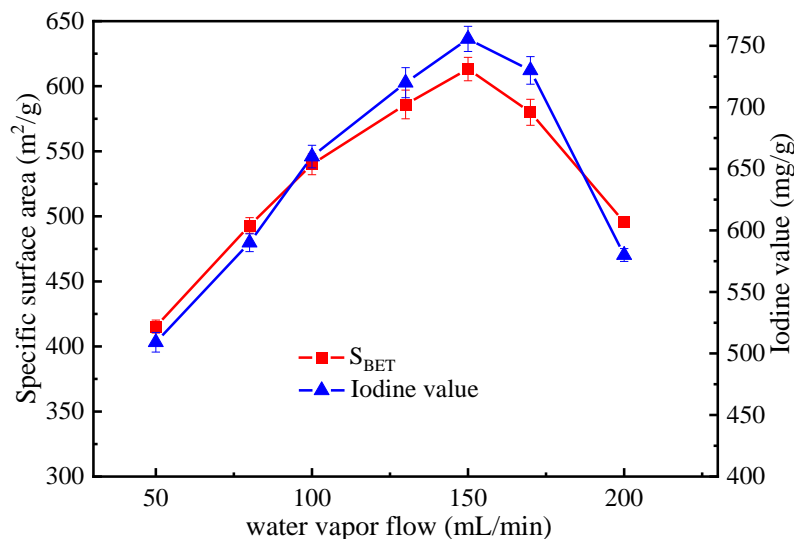


Figure 6. Effect of steam flow on the textural property of the obtained sample.

3.2.4. Surface Properties of the Obtained Activated Carbon

The morphologies of the raw material SC and the activated carbon obtained at the optimal preparation conditions were monitored via SEM. As presented in Figure 7, it was clear that there were few pores in the raw material SC, while the structures of the activated carbon obtained at the optimal preparation condition possessed lots of micropores and mesopores, which was beneficial to CO₂ adsorption.

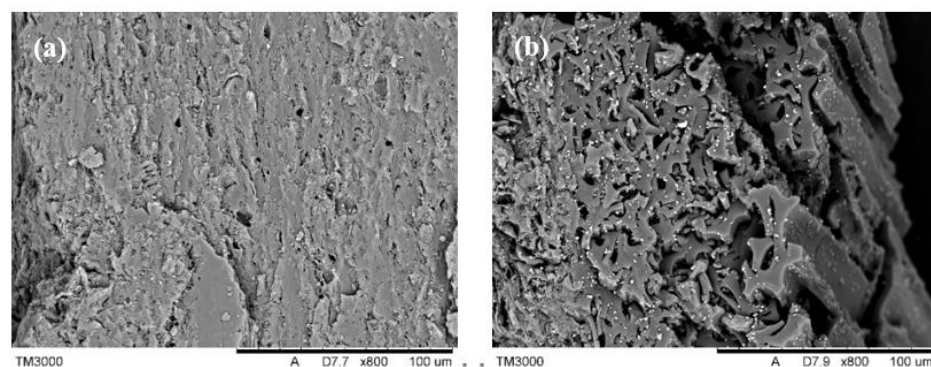


Figure 7. SEM of (a) pulverized semi-coke; (b) AC-700-70-150.

3.3. CO₂ Sorption Performance of the Obtained Activated Carbon

Table 3 summarizes the CO₂ sorption capacity of the samples. It was evaluated at 40 °C and 50 °C with different CO₂ partial pressures under local atmospheric pressure. These samples were prepared in different activation conditions. The above analysis showed that the activation conditions could directly affect the pore structure of activated carbon, which further affected the CO₂ sorption capacity. Researchers found that under atmospheric

pressure, the CO₂ sorption capacity was proportional to the pore volume of pore sizes of less than 8 nm. However, the samples with the highest specific surface area or the maximum pore volume did not show the best CO₂ sorption capacity [34]. In this work, activated carbon obtained by employing 150 mL/min steam to treat pulverized semi-coke at 700 °C for 70 min (AC-700-70-150) had the highest micropore ratio of 0.83 and the maximum iodine value of 755.6 mg/g (Table 1), which indicated that the adsorbent AC-700-70-150 had the most developed micropore structure [20,25,35]. It can be seen from Table 3 that the AC-700-70-150 showed the highest CO₂ sorption capacity of 1.80 mmol/g at 40 °C when the CO₂ partial pressure was 90 kPa. When the CO₂ partial pressure was low, the micropores with a smaller pore size mainly contributed to the CO₂ sorption capacity. Therefore, the CO₂ sorption capacity of adsorbents decreased under lower CO₂ partial pressure. When the CO₂ partial pressure reduced to 15 kPa, the CO₂ sorption capacity of AC-700-70-150 decreased to 0.85 mmol/g. The adsorption between carbon sorbents and CO₂ was typical for physisorption processes. As the adsorption temperature increased, the CO₂ sorption capacity of samples decreased.

Table 3. CO₂ sorption capacity of the obtained activated carbon.

Sample	CO ₂ Sorption Capacity (mmol/g)		
	40 °C		50 °C
	15 kPa	90 kPa	90 kPa
AC-650-50-150	0.24	1.09	0.74
AC-680-50-150	0.47	1.41	1.26
AC-700-50-150	0.62	1.65	1.32
AC-750-50-150	0.4	1.33	1.18
AC-800-50-150	0.35	1.28	1.07
AC-700-30-150	0.25	1.13	0.85
AC-700-70-150	0.85	1.80	1.54
AC-700-90-150	0.38	1.31	1.14
AC-700-70-50	0.33	1.25	1.07
AC-700-70-100	0.51	1.49	1.25
AC-700-70-200	0.47	1.42	1.26

The commercial activated carbon was selected as a comparison to estimate the CO₂ sorption capacity of the activated carbon prepared from pulverized semi-coke under the same experimental condition. The CO₂ sorption capacity of two activated carbons at different temperatures with 15 vol% CO₂ partial pressure is summarized in Figure 8. As the temperature increased, the CO₂ sorption capacity of both activated carbons showed a declining trend. When the adsorbed temperature was 20 °C or 30 °C, the CO₂ sorption capacity of two kinds of activated carbons were similar. However, when the temperature was elevated to 40 °C, the CO₂ sorption capacity of the activated carbon prepared from pulverized semi-coke (AC-700-70-150) was obviously higher than that of the commercial activated carbon (AC-Commercial). At low temperatures, physical adsorption was carried out between activated carbon and CO₂. The pore structure of activated carbon greatly influences CO₂ sorption performance. Therefore, the pore structure of the two kinds of activated carbons was determined, and the results are shown in Table 4. It was obvious that there were more micropores in AC-700-70-150. Though the BET surface area of commercial activated carbon was larger than that of AC-700-70-150 derived from pulverized semi-coke, the CO₂ sorption capacity did not follow the same trend. Some works indicated that the CO₂ sorption capacity of adsorbents was not positively correlated with their BET surface area but correlated with the pore size distribution [36,37]. Compared to commercial activated carbon, AC-700-70-150 had a higher micropore ratio of 0.83. Furthermore, the properties of activated carbon, especially pore size distribution, played a decisive role in the CO₂ sorption performance of activated carbon. Figure 9 compares the DFT pore size distribution of AC-700-70-150 and commercial activated carbon. The pore size of AC-700-

70-150 was mostly 0.55 nm, while the commercial activated carbon obtained a pore size of 1.41 nm. The CO₂ molecular kinetic diameter was 0.33 nm; when the pore size of adsorbent was 2–3 times the molecular kinetic diameter of CO₂, the adsorbent presented good CO₂ sorption performance [34]. This indicated that pore sizes of smaller than 1 nm were more favorable to CO₂ sorption. Thus, though the BET surface area of AC-700-70-150 derived from pulverized semi-coke was smaller than that of the commercial activated carbon, due to its smaller pore size of 0.55 nm, AC-700-70-150 possessed good CO₂ sorption capacity, especially at a higher adsorbed temperature.

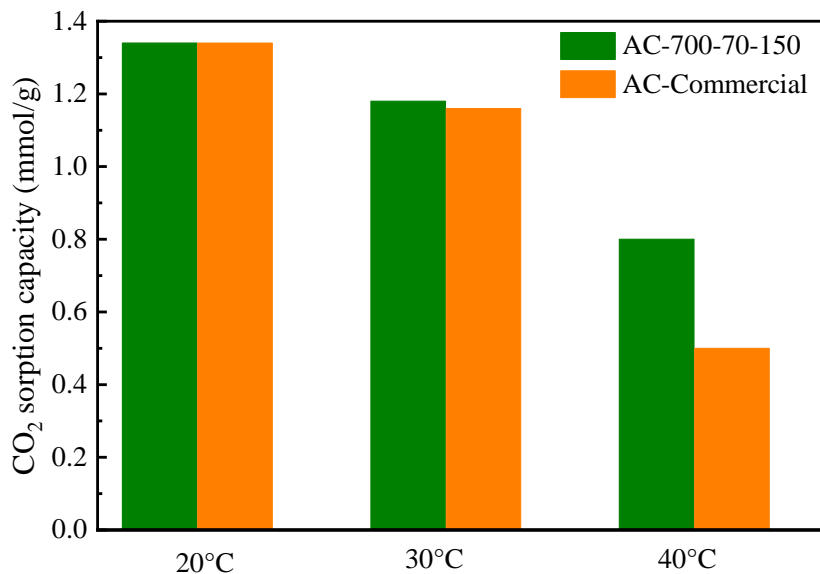


Figure 8. The CO₂ adsorption performance of two kinds of activated carbons at different temperatures.

Table 4. Textural properties of AC-700-70-150 and commercial activated carbon.

Sample	S _{BET} (m ² /g)	V _t (cm ³ /g)	V _{mic} (cm ³ /g)	Ratio V _{mic} :V _t	Pore Size (nm)
AC-Commercial	870.4	0.48	0.22	0.46	1.41
AC-700-70-150	590.2	0.29	0.24	0.83	0.55

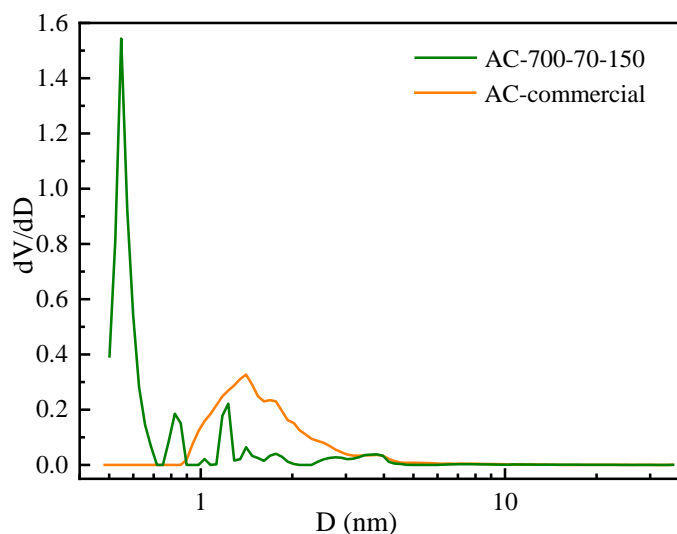


Figure 9. DFT pore-size distribution of AC-700-70-150 and commercial activated carbon.

Since AC-700-70-150 possessed the highest CO₂ sorption capacity, we selected AC-700-70-150 for cyclic adsorption/desorption experiments at 40 °C for simulating the post-combustion sorption process. In order to explore the selectivity of CO₂/N₂ of the AC-700-70-150, we also investigated its sorption properties in pure N₂ at the same experimental condition. Results are summarized in Figure 10. When the sample was exposed to a pure N₂ atmosphere, the mass uptake in sorption stage was only about 0.4% (equivalent to 0.14 mmol N₂/g sorbent). When the feed gas was 15% CO₂ in N₂, the mass uptake in the adsorption stage was 3.6% (equivalent to 0.85 mmol CO₂/g sorbent). Furthermore, it can be seen that the mass uptake during the sorption stage was equal to the mass loss during the desorption stage, indicating that the CO₂ sorption capacity of AC-700-70-150 was steady during the five cycles. Besides, its CO₂/N₂ selectivity was 34.4, which was higher than that of ZIF [38]. Thus, AC-700-70-150 derived from pulverized semi-coke obtained good selectivity at low partial pressure.

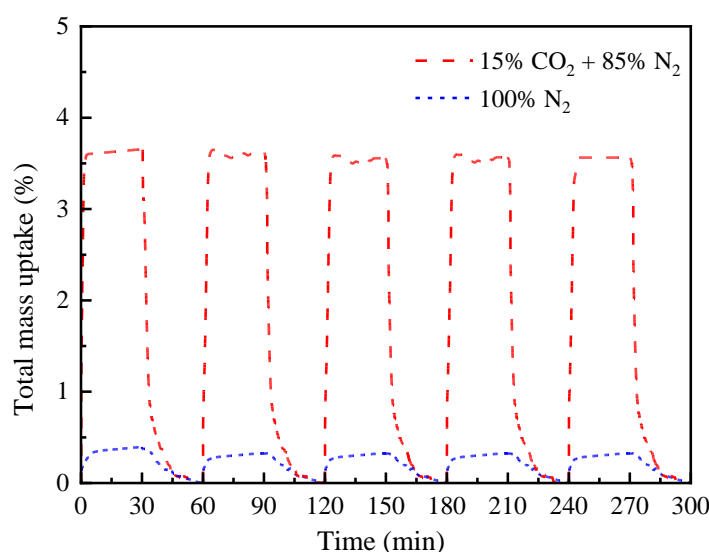


Figure 10. Sorption/desorption performance of AC-700-70-150.

4. Conclusions

Microporous activated carbons were prepared from pulverized semi-coke through steam activation. The influence of the demineralization and activation conditions on the structure and performance of the synthesized activated carbon was investigated. The results indicated that demineralization with acid before activation contributed to the formation of micropores. The optimal activation condition for preparing activated carbon was an activation temperature of 700 °C, activation time of 70 min and steam flow of 150 mL/min. When the obtained activated carbon was evaluated as a CO₂ sorbent, due to the physical sorption between activated carbon and CO₂, the CO₂ sorption capacity varied by sorption temperature and pressure, and the highest CO₂ sorption capacity of 1.80 mmol/g was obtained at 40 °C when the CO₂ partial pressure was 90 kPa. Compared with commercial activated carbon, AC-700-70-150 derived from pulverized semi-coke obtained a good CO₂/N₂ selectivity of 34.4 and its CO₂ sorption capacity was steady during the five cycles. Combined with the analysis of textural properties of the samples, the superior CO₂ sorption performance of AC-700-70-150 was attributed to its narrow pore size distribution, and it was found that a pore size of smaller than 1 nm was more favorable for CO₂ sorption.

Author Contributions: Conceptualization, J.J.; data curation, Z.Z. and X.Z.; funding acquisition, J.J.; project administration, J.J.; supervision, J.J.; writing—original draft, Z.Z. and X.Z.; writing—review and editing, J.J., J.F. and W.L. All authors have read and agreed to the published version of the manuscript.

Funding: This research was funded by National Key Research and Development Program of China (grant number: 2019YFC1906804-03), Shanxi-Zheda Institute of Advanced Materials and Chemical Engineering (grant number: 2021SX-FR002) and the Fund for Shanxi 1331 Project (No grant number). And the APC was funded by the above grants.

Institutional Review Board Statement: Not applicable.

Informed Consent Statement: Not applicable.

Data Availability Statement: Not applicable.

Conflicts of Interest: The authors declare no conflict of interest.

References

1. Chai, S.Y.W.; Ngu, L.H.; How, B.S. Review of carbon capture absorbents for CO₂ utilization. *Greenh. Gases* **2022**, *12*, 394–427. [[CrossRef](#)]
2. Dunstan, M.T.; Donat, F.; Bork, A.H.; Grey, C.P.; Muller, C.R. CO₂ capture at medium to high temperature using solid oxide-based sorbents: Fundamental aspects, mechanistic insights, and recent advances. *Chem. Rev.* **2021**, *121*, 12681–12745. [[CrossRef](#)] [[PubMed](#)]
3. Aghel, B.; Janati, S.; Alobaid, F.; Almoslh, A.; Epple, B. Application of nanofluids in CO₂ absorption: A review. *Appl. Sci.* **2022**, *12*, 3200. [[CrossRef](#)]
4. Aghel, B.; Behaein, S.; Wongwises, S.; Shadloo, M.S. A review of recent progress in biogas upgrading: With emphasis on carbon capture. *Biomass Bioenergy* **2022**, *160*, 106422. [[CrossRef](#)]
5. Plaza, M.G.; Thurecht, K.J.; Pevida, C.; Rubiera, F.; Pis, J.J.; Snape, C.E.; Drage, T.C. Influence of oxidation upon the CO₂ capture performance of a phenolic-resin-derived carbon. *Fuel Process. Technol.* **2013**, *110*, 53–60. [[CrossRef](#)]
6. Wang, P.; Guo, Y.F.; Zhao, C.W.; Yan, J.J.; Lu, P. Biomass derived wood ash with amine modification for post-combustion CO₂ capture. *Appl. Energy* **2017**, *201*, 34–44. [[CrossRef](#)]
7. Chan, W.H.; Mazlee, M.N.; Ahmad, Z.A.; Ishak, M.A.M.; Shamsul, J.B. The development of low cost adsorbents from clay and waste materials: A review. *J. Mater. Cycles Waste Manag.* **2017**, *19*, 1–14. [[CrossRef](#)]
8. Aghel, B.; Janati, S.; Wongwises, S.; Shadloo, M.S. Review on CO₂ capture by blended amine solutions. *Int. J. Greenh. Gas Cont.* **2022**, *119*, 103715. [[CrossRef](#)]
9. Rozaidin, S.A.M.; Lau, K.K. A review on enhancing solvent regeneration in CO₂ absorption process using nanoparticles. *Sustainability* **2022**, *14*, 4750. [[CrossRef](#)]
10. Ooi, Z.L.; Tan, P.Y.; Tan, L.S.; Yeap, S.P. Amine-based solvent for CO₂ absorption and its impact on carbon steel corrosion: A perspective review. *Chin. J. Chem. Eng.* **2020**, *28*, 1357–1367. [[CrossRef](#)]
11. Bravo, J.; Drapanauskaite, D.; Sarunac, N.; Romero, C.; Jesikiewicz, T.; Baltrusaitis, J. Optimization of energy requirements for CO₂ post-combustion capture process through advanced thermal integration. *Fuel* **2021**, *283*, 118940. [[CrossRef](#)]
12. Dong, B.X.; Zhang, S.Y.; Liu, W.L.; Wu, Y.C.; Ge, J.; Song, L.; Teng, Y.L. Gas storage and separation in water-stable [Cu₅BTT₃]⁴⁻ anion framework comprising giant multi-prismatic nanoscale cage. *Chem. Commun.* **2015**, *51*, 5691–5694. [[CrossRef](#)] [[PubMed](#)]
13. Rashidi, N.A.; Yusup, S. An overview of activated carbons utilization for the post-combustion carbon dioxide capture. *J. CO₂ Util.* **2016**, *13*, 1–16. [[CrossRef](#)]
14. Creamer, A.E.; Gao, B. Carbon-based adsorbents for postcombustion CO₂ capture: A critical review. *Environ. Sci. Technol.* **2016**, *50*, 7276–7289. [[CrossRef](#)]
15. Wang, J.; Pu, Q.; Ning, P.; Lu, S. Activated carbon-based composites for capturing CO₂: A review. *Greenh. Gases* **2021**, *11*, 377–393. [[CrossRef](#)]
16. Karami, F.; Aghel, B.; Moradi, P.; Karimi, M. Stripping of hydrogen sulfide from crude oil desalter effluent via different adsorbents. *Int. J. Environ. Sci. Technol.* **2022**, *19*, 5119–5130. [[CrossRef](#)]
17. Serafin, J.; Narkiewicz, U.W.; Morawski, A.; Wróbel, R.J.; Michalkiewicz, B. Highly microporous activated carbons from biomass for CO₂ capture and effective micropores at different conditions. *J. CO₂ Util.* **2017**, *18*, 73–79. [[CrossRef](#)]
18. Wang, J.; Lei, S.; Liang, L. Preparation of porous activated carbon from semi-coke by high temperature activation with KOH for the high-efficiency adsorption of aqueous tetracycline. *Appl. Surf. Sci.* **2020**, *530*, 147187. [[CrossRef](#)]
19. Tian, H.; Pan, J.; Zhu, D.; Guo, Z.; Yang, C.; Xue, Y.; Li, S.; Wang, Y. Innovative one-step preparation of activated carbon from low-rank coals activated with oxidized pellets. *J. Clean. Prod.* **2021**, *313*, 127877. [[CrossRef](#)]
20. Heidarinejad, Z.; Dehghani, M.H.; Heidari, M.; Javedan, G.; Ali, I.; Sillanpää, M. Methods for preparation and activation of activated carbon: A review. *Environ. Chem. Lett.* **2020**, *18*, 393–415. [[CrossRef](#)]
21. Plaza, M.G.; González, A.S.; Pevida, C.; Pis, J.J.; Rubiera, F. Valorisation of spent coffee grounds as CO₂ adsorbents for postcombustion capture applications. *Appl. Energy* **2012**, *99*, 272–279. [[CrossRef](#)]
22. Li, B.F.; Li, X.H.; Li, W.Y.; Feng, J. Co-pyrolysis performance of coal and its direct coal liquefaction residue with solid heat carrier. *Fuel Process. Technol.* **2017**, *166*, 69–76. [[CrossRef](#)]
23. Ye, C.P.; Yang, Z.J.; Li, W.Y.; Rong, H.L.; Feng, J. Effect of adjusting coal properties on HulunBuir lignite pyrolysis. *Fuel Process. Technol.* **2017**, *156*, 415–420. [[CrossRef](#)]

24. Pradhan, B.K.; Sandle, N.K. Effect of different oxidizing agent treatments on the surface properties of activated carbons. *Carbon* **1999**, *37*, 1323–1332. [[CrossRef](#)]
25. Bjornerback, F.; Hedin, N. Microporous humins prepared from sugars and bio-based polymers in concentrated sulfuric acid. *ACS Sust. Chem. Eng.* **2019**, *7*, 1018–1027. [[CrossRef](#)]
26. Ao, W.; Fu, J.; Mao, X.; Kang, Q.; Ran, C.; Liu, Y.; Zhang, H.; Gao, Z.; Li, J.; Liu, G.; et al. Microwave assisted preparation of activated carbon from biomass, A review. *Renew. Sust. Energy Rev.* **2018**, *92*, 958–979. [[CrossRef](#)]
27. Lai, J.Y.; Ngu, L.H.; Hashim, S.S. A review of CO₂ adsorbents performance for different carbon capture technology processes conditions. *Greenh. Gases* **2021**, *11*, 1076–1117. [[CrossRef](#)]
28. Martín, C.F.; Plaza, M.G.; Pis, J.J.; Rubiera, F.; Pevida, C.; Centeno, T.A. On the limits of CO₂ capture capacity of carbons. *Sep. Purif. Technol.* **2010**, *74*, 225–229. [[CrossRef](#)]
29. Murakami, T.; Xu, G.; Suda, T.; Matsuzawa, Y.; Tani, H.; Fujimori, T. Some process fundamentals of biomass gasification in dual fluidized bed. *Fuel* **2007**, *86*, 244–255. [[CrossRef](#)]
30. Alauddin, Z.A.B.Z.; Lahijani, P.; Mohammadi, M.; Mohamed, A.R. Gasification of lignocellulosic biomass in fluidized beds for renewable energy development: A review. *Renew. Sust. Energy Rev.* **2010**, *14*, 2852–2862. [[CrossRef](#)]
31. Chen, D.; Chen, X.; Sun, J.; Zheng, Z.; Fu, K. Pyrolysis polygeneration of pine nut shell: Quality of pyrolysis products and study on the preparation of activated carbon from biochar. *Bioresour. Technol.* **2016**, *216*, 629–636. [[CrossRef](#)] [[PubMed](#)]
32. Poinern, G.; Senanayake, G.; Shah, N.; Thile, X.; Parkinson, G.; Fawcett, D. Adsorption of the aurocyanide, Au(CN)₂[−] complex on granular activated carbons derived from macadamia nut shells: A preliminary study. *Miner. Eng.* **2011**, *24*, 1694–1702. [[CrossRef](#)]
33. Campoy, M.; Gómez-Barea, A.; Vidal, F.B.; Ollero, P. Air–steam gasification of biomass in a fluidised bed: Process optimisation by enriched air. *Fuel Process. Technol.* **2009**, *90*, 677–685. [[CrossRef](#)]
34. Presser, V.; McDonough, J.; Yeon, S.H.; Gogotsi, Y. Effect of pore size on carbon dioxide sorption by carbide derived carbon. *Energy Environ. Sci.* **2011**, *4*, 3059–3066. [[CrossRef](#)]
35. Fu, J.; Zhou, B.; Zhang, Z.; Wang, T.; Cheng, X.; Lin, L.; Ma, C. One-step rapid pyrolysis activation method to prepare nanostructured activated coke powder. *Fuel* **2020**, *262*, 116514. [[CrossRef](#)]
36. Marco-Lozar, J.P.; Kunowsky, M.; Suárez-García, F.; Linares-Solano, A. Sorbent design for CO₂ capture under different flue gas conditions. *Carbon* **2014**, *72*, 125–134. [[CrossRef](#)]
37. Ben-Mansour, R.; Habib, M.A.; Bamidele, O.E.; Basha, M.; Qasem, N.A.A.; Peedikakkal, A.; Laoui, T.; Ali, M. Carbon capture by physical adsorption: Materials, experimental investigations and numerical modeling and simulations—A review. *Appl. Energy* **2016**, *161*, 225–255. [[CrossRef](#)]
38. Valencia, L.; Abdelhamid, H.N. Nanocellulose leaf-like zeolitic imidazolate framework (ZIF-L) foams for selective capture of carbon dioxide. *Carbohydr. Polym.* **2019**, *213*, 338–345. [[CrossRef](#)]